Field Crops Research 214 (2017) 239–252

Contents lists available at ScienceDirect

Field Crops Research

journal homepage: www.elsevier.com/locate/fcr

Modeling the response of maize phenology, kernel set, and yield components to heat stress and heat shock with CSM-IXIM

J.I. Lizaso[a,*], M. Ruiz-Ramos[a], L. Rodríguez[a], C. Gabaldon-Leal[b], J.A. Oliveira[c], I.J. Lorite[b], A. Rodríguez[a,d], G.A. Maddonni[e], M.E. Otegui[f]

[a] CEIGRAM-Universidad Politécnica de Madrid, ETSIAAB, 28040, Madrid, Spain
[b] IFAPA-Centro Alameda del Obispo, Junta de Andalucía, P.O. Box 3092, 14080, Córdoba, Spain
[c] Área de Producción Vegetal, Universidad de Oviedo, EPM, 33600, Mieres, Spain
[d] University of Castilla-La Mancha, Department of Economic Analysis, Toledo, Spain
[e] IFEVA-CONICET, Facultad de Agronomía, Universidad de Buenos Aires, Argentina
[f] CONICET-INTA, Facultad de Agronomía, Universidad de Buenos Aires, Argentina

ARTICLE INFO

Keywords:
Heat stress
Maize
CSM-IXIM
CSM-CERES-maize
Beta function

ABSTRACT

The available evidence suggests that the current increasing trend in global surface temperatures will continue during this century, which will be accompanied by a greater frequency of extreme events. The IPCC has projected that higher temperatures may outscore the known optimal and maximum temperatures for maize. The purpose of this study was to improve the ability of the maize model CSM-IXIM to simulate crop development, growth, and yield under hot conditions, especially with regards to the impact of above-optimal temperatures around anthesis. Field and greenhouse experiments that were performed over three years (2014–2016) using the same short-season hybrid, PR37N01 (FAO 300), provided the data for this work. Maize was sown at a target population density of 5 plants m^{-2} on two sowing dates in 2014 and 2015 and on one in 2016 at three locations in Spain (northern, central, and southern Spain) with a well-defined thermal gradient. The same hybrid was also sown in two greenhouse chambers with daytime target temperatures of approximately 25 and above 35 °C. During the nighttime, the temperature in both chambers was allowed to equilibrate with the outside temperature. The greenhouse treatments consisted of moving 18 plants at selected phenological stages (V4, V9, anthesis, lag phase, early grain filling) from the cool chamber to the hot chamber over a week and then returning the plants back to the cool chamber. An additional control treatment remained in the cool chamber all season, and in 2015 and 2016, one treatment remained permanently in the hot chamber. Two maize models in the Decision Support System for Agrotechnology Transfer (DSSAT) V4.6 were compared, namely CERES and IXIM. The IXIM version included additional components that were previously developed to improve the crop N simulation and to incorporate the anthesis-silking interval (ASI). A new thermal time calculation, a heat stress index, the impact of pollen-sterilizing temperatures, and the explicit simulation of male and female flowering as affected by the daily heat conditions were added to IXIM. The phenology simulation in field experiments by IXIM improved substantially. The RMSE for silking and maturity in CERES were 7.9 and 13.7 days, decreasing in IXIM to 2.8 and 7.3 days, respectively. Similarly, the estimated kernel numbers, kernel weight, grain yield and final biomass were always closer to the measurements in IXIM than in CERES. The worst simulations were for kernel weight, and for that reason, the differences in grain yield between the models were small (the RMSE in CERES was 1219 kg ha^{-1} *vs.* 1082 kg ha^{-1} in IXIM). The greenhouse results also supported the improved estimations of crop development by IXIM (RMSE of 2.6 days) relative to CERES (7.4 days). The impact of the heat treatments on grain yield was consistently overestimated by CERES, while IXIM captured the general trend. The new IXIM model improved the CERES simulations when elevated temperatures were included in the evaluation data. Additional model testing with measurements from a wider latitudinal range and relevant heat conditions are required.

* Corresponding author.
E-mail address: jon.lizaso@upm.es (J.I. Lizaso).

http://dx.doi.org/10.1016/j.fcr.2017.09.019
Received 23 June 2017; Received in revised form 7 September 2017; Accepted 11 September 2017

1. Introduction

The intergovernmental panel on climate change (IPCC) summarized the current understanding of climate projections for a broad set of emissions scenarios. The surface of our home planet will likely continue experiencing temperature increases in many highly populated maize cropping regions through the present century, with more frequent and intense heat waves (IPCC, 2014). These trends imply that future efforts to increase food production will in most places be under warmer conditions and will be affected by frequent extreme temperatures. They also note the need to improve our predictive tools to estimate the impact of heat accurately on our major food crops, such as maize (*Zea mays* L), which is the cereal crop with the highest global production level (FAO, 2014).

Simulation models use a number of temperature functions to capture the responses of crop processes to the thermal environment. Most of these functions depict an accelerated rate with a temperature increase over a range of temperatures described as suboptimum, followed by a decreasing rate at temperatures above the optimum (*i.e.*, supraoptimal; Parent and Tardieu, 2012). Kumudini et al. (2014) compared several of these functions representing the developmental responses to temperature. They found the best predictive capacity using Crop Heat Units (CHU, Brown and Bootsma, 1993) and the General Thermal Index (GTI, Stewart et al., 1998). The CHU system was developed for maize in southern Ontario (Brown, 1969), and then it was extended to other crops and regions in Canada. The GTI system was developed using field data collected at latitudes 39–48° N, with mean temperatures within a 10–30 °C range. Both functions must still be tested at supraoptimal temperatures. The CHU system uses a daytime and a nighttime function that are calculated from maximum and minimum temperatures, and then both values are averaged to calculate a daily CHU figure. The thermal time calculated by the CHU system (Fig. 1a) depends on the daily thermal amplitude (Amp); the greater the amplitude, the lower the optimum temperature and the estimated thermal time. The GTI system (Fig. 1b) uses two distinct polynomial functions for the vegetative and reproductive phases. The shape of the function for the vegetative phase is quite similar to that of the simplified beta function, with optimum and maximum temperatures of 32.2 and 48.3 °C respectively. The function for the reproductive phase is a quadratic polynomial with no optimum temperature.

Parent and Tardieu (2012) described the development rate response to the temperature in 17 crop species including 8 inbreds and one maize hybrid. The authors normalized the rates using the corresponding average values at 20 °C and fitted an Arrhenius function to the data sets (Parent et al., 2010). In spite of the large diversity of genotypes examined here, the normalized responses of the maize development rate to the temperature were surprisingly concordant, increasing gradually until an optimum temperature of approximately 30 °C and decreasing thereafter at a sharp rate. The simplified beta function (Yan and Hunt, 1999) also captured a number of maize developmental processes with a similar shape, with optimum temperatures between 29.7 and 32.6 °C. Therefore, the latter function was a simple option to describe the response of the maize development rate to the temperature, and to estimate the durations of the maize phases in thermal time units with three meaningful parameters.

Several studies have documented the effects of extremely high temperatures (*i.e.*, heat) on the biomass production, floral development, and kernel set in maize crops. Heat stress affects biomass production, and it is linked to variations in the radiation use efficiency and the amount of light captured by crops (Rattalino-Edreira and Otegui, 2012). The latter is due to the shortening effect of heat on the cycle duration. Heat stress also reduces pollen shed (Schoper et al., 1987) and pollen viability (Herrero and Johnson, 1980; Mitchell and Petolino, 1988). Silk extrusion is also affected by heat imposed immediately before female flowering (Cicchino et al., 2010b; Rattalino-Edreira et al., 2011; Ordoñez et al., 2015). Even when pistils are pollinated with fertile pollen, the kernel abortion of fertilized flowers dramatically affects the kernel set (Rattalino-Edreira and Otegui, 2013).

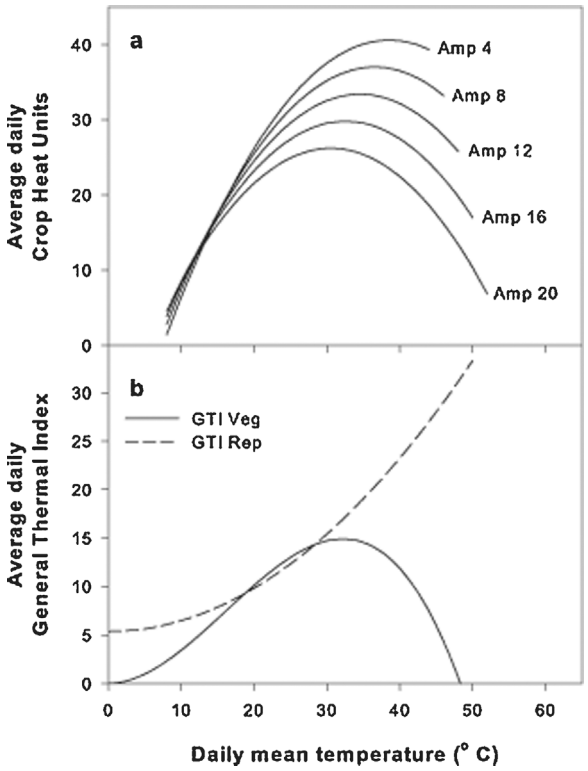

Fig. 1. Two proposed procedures to estimate the thermal time. a: The Crop Heat Units (CHU, Brown and Bootsma, 1993) calculates a daytime value from the daily maximum temperature and a nighttime value from the daily minimum temperature. The CHU is the average of both values. Depending on the daily thermal amplitude (Amp °C), different responses (*i.e.*, thermal times) are estimated. b: The General Thermal Index (GTI, Stewart et al., 1998) estimates two different responses for the vegetative and the reproductive phases, with no maximum for the reproductive phase.

Maize simulation models, such as those in the DSSAT, do not incorporate the explicit simulation of heat affecting male and female flowering, the fertilization of female flowers, and kernel abortion. For that reason, Sánchez et al. (2014) concluded that crop models are too optimistic to predict the effects of global warming on crop production. The objective of this work was to improve the ability of CSM-IXIM, one of the maize models available in DSSAT, to simulate heat stress effects on crop development, growth, and grain yield. For that purpose, we used CERES-Maize as a benchmark to evaluate the performance of CSM-IXIM (the original and the new IXIM versions are not compared in this paper).

2. Materials and methods

2.1. Data collection

2.1.1. Field experiments

Data to support this work were provided by field and greenhouse experiments (Lizaso et al., 2017, this special issue). The maize (*Zea mays* L.) hybrid PR37N01 was grown at a target stand density of 5 plants m^{-2} at three sites in Spain along a north-south thermal gradient. The locations were Candás in the north (Latitude: 43.58 N; Longitude: 5.78 W; Elevation: 80 m), Aranjuez in the center (Latitude: 40.06 N; Longitude: 3.54 W; Elevation: 525 m), and Córdoba in the south (Latitude: 37.86 N; Longitude: 4.79 W; Elevation: 117 m). In 2014 and 2015, two sowing dates were used at each site, and only one was used in 2016 (see details in Table 1 in Lizaso et al., 2017, this special issue, and in suppl. mat. in Table S1 this paper). Sprinkler irrigation was applied to

Table 1
Greenhouse treatments for 2014, 2015 and 2016. The treatments were identified as follows: plants in the cool chamber for the entire crop cycle or the control (C), heat at V4 (V4), in the cool chamber up to V4 and then they were moved to the hot chamber (V4c), in the hot chamber up to V4 and then they were moved to the cool chamber (V4 h), heat at V9 (V9), heat at anthesis (FL), heat at lag phase (LG), heat at early grain filling (GF), heat-all crop cycle (H), growing in the cool chamber and pollinated with pollen from the hot chamber (C x H), and growing in the hot chamber and pollinated with pollen from the cool chamber (H x C).

Year:	2014	2015	2016
Treatment:	C	C	C
	V4	V4	V4c
	V9	V9	V9
	FL	FL	FL
	LG	LG	LG
	GF	GF	V4h
		H	H
			C × H
			H × C

maintain adequate soil moisture throughout the season. Pre-season soil sampling provided information to calculate the fertilizer requirements for optimum growth. Pests, diseases and weeds were controlled effectively.

2.1.2. Greenhouse experiments

The two greenhouse chambers, cool and hot, differed in their target daytime temperature (25 °C in the cool chamber, and above 35 °C in the hot chamber), and they provided controlled environments to complement the information for this work. Late in the afternoon, the heating and cooling systems were switched off and the windows were opened, allowing both chambers to equilibrate with the outside temperatures. The same hybrid used in the field experiments was sown in 15-L pots in late May or early June during 2014–2016. The pots were irrigated twice a day and fertilized weekly. The experimental unit consisted of three plants and was replicated three times, with two pollen sources used for pollination for a total of 18 plants per treatment. The plants from each treatment were always together in the same chamber. All the topmost ears were hand-pollinated once at mid-morning three days after silking, with half taking pollen from the same treatment and half with fresh pollen collected in a nearby field to separate the effects of the heat on the male and female components. The heat treatments consisted of moving 18 plants of the corresponding treatment from the cool chamber to the hot chamber and returning the plants back to the cool chamber seven days later. Heat treatments were applied at specific phenological times, and they are specified in Table 1 (see details in Lizaso et al., 2017, this special issue).

2.2. Describing current models

2.2.1. Crop phenology

Two maize models distributed with DSSAT V4.6 version 4.6.0.039 (Hoogenboom et al., 2015), CSM-CERES-Maize (hereafter CERES) and CSM-IXIM (hereafter IXIM) were compared in this study. Both models have similar temperature response functions for phenology and seed growth, and neither model explicitly simulates the impact of heat stress on the kernel set and grain yield. The IXIM version used here (see section "*Additional components in IXIM*") included two recent developments, i) the new estimation of crop N demand and partitioning (Yakoub et al., 2017) and ii) the simulation of the anthesis-silking interval (current work). Both models, CERES and IXIM, estimated the progress throughout the crop life cycle by accumulating the thermal time that was calculated linearly from the daily mean temperature with base and optimum temperatures of 8 and 34 °C, respectively. Above-optimal temperatures will maintain a constant thermal time as at 34 °C. The duration of phenological phases is controlled by cultivar-specific coefficients. The only exception is the floral induction phase, which lasts 4 days, but over long days (*i.e.*, longer than 12.5 h), the duration can be extended for photoperiod-sensitive cultivars.

2.2.2. Crop growth

CERES (Jones and Kiniry, 1986) estimates the per-plant leaf area and PAR interception and then calculates the daily plant growth rate using the radiation use efficiency (RUE) approach. The most limiting growing condition associated with the daytime temperature, soil water, and nutrients reduces the calculated daily plant growth rate using the most limiting zero-to-one stress coefficient.

IXIM (Lizaso et al., 2011) describes on a per-leaf basis, leaf surface, PAR capture, instantaneous leaf CO_2 assimilation, and, using the tissue composition, it estimates the canopy respiration and finally the plant growth rate. The hourly temperatures, which are extrapolated according to Parton and Logan (1981), influence the photosynthetic rate (Oberhuber and Edwards, 1993) and maintenance respiration (McCree, 1974) when calculating the growth rate (Lizaso et al., 2005).

2.2.3. Grain yield

CERES calculates grain yield by adding the daily product of the kernel number and kernel growth rate during the effective grain-filling phase. The kernel number is calculated with a modification of the Edmeades and Daynard (1979) relationship. During the post-silking lag phase, an average daily plant growth rate is calculated and converted into a daily photosynthetic rate. A linear function with a maximum is used, instead of the original curvilinear relationship (Edmeades and Daynard, 1979), to estimate the number of grains per plant (Fig. 2). Both the maximum kernel number and the kernel growth rate are cultivar-specific parameters. The daily growth of grain may be reduced by inadequate temperatures and limited soil water, by incorporating a zero-to-one function of the daily mean temperature and a function of the water stress, if any. The temperature function assumes a range of mean temperatures (default 16–27 °C) for optimum kernel growth, with minimum and maximum mean temperatures (with defaults of 5.5 and 35 °C, respectively) at which kernel growth stops (Jones and Kiniry, 1986; Ritchie et al., 1998).

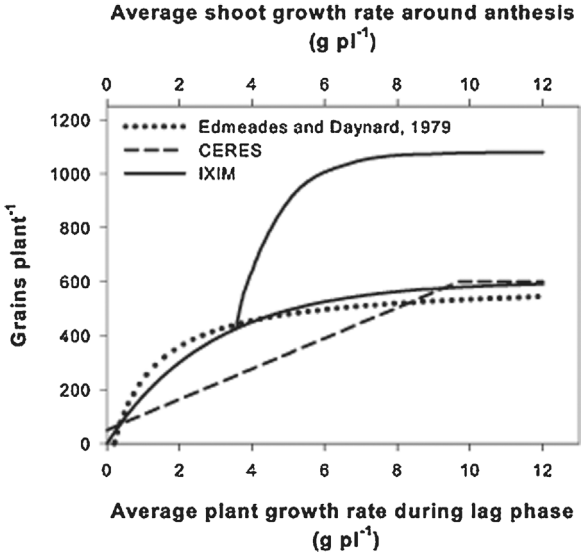

Fig. 2. Functions to estimate the plant kernel number as a function of the source of assimilates according to Edmeades and Daynard (1979), dotted line; current CERES model (modified from Jones and Kiniry, 1986), dashed line; and original IXIM model (Lizaso et al., 2011), solid line, double curve. The function by Edmeades and Daynard uses the reverse conversion used by CERES, both as a function of the plant growth rate. IXIM estimates the cumulative kernels in the apical (lower curve) and sub-apical (upper curve) ears as a function of the shoot growth rate. All the functions are calculated by assuming a maximum kernel number (G2, Table 5) of 600 seeds plant^{-1}.

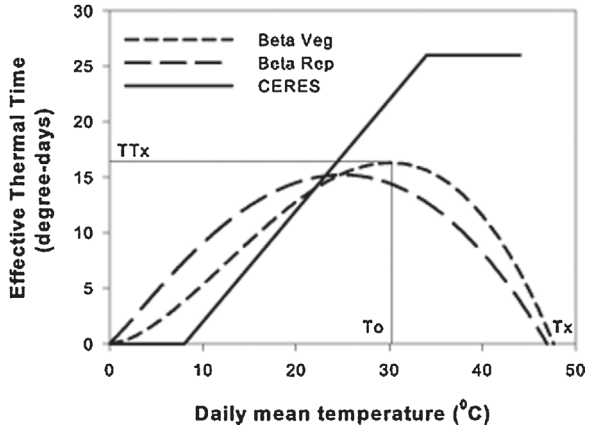

Fig. 3. Comparison of functions to estimate the thermal time by CERES, a solid line; and the optimized beta function for vegetative (Beta-Veg), and reproductive (Beta-Rep) phases, dashed lines. The parameters of the beta function (Table 3) are indicated as follows: optimum (*To*) and maximum (*Tx*) temperatures, and maximum thermal time (*TTx*) at the optimum temperature.

IXIM uses a different approach to calculate the kernel number. It defines a critical thermal time window around silking (with a default of 250 growing degree-days, or GDD, before silking, through 100 GDD after silking) and determines an average shoot growth rate. With this average shoot growth rate, a double curve estimates the cumulative number of kernels in apical (lower curve) and sub-apical (upper curve) ears (Fig. 2). Similar to CERES, the daily kernel growth uses a temperature function but no water stress function, because the shoot growth rate is already affected by water deficits (Lizaso et al., 2011).

2.3. Incorporating heat stress into IXIM

2.3.1. Improving the simulation of maize phenology

The duration of phenological phases is affected by the temperature, with both sub and supraoptimal temperatures extending the duration (Challinor et al., 2005). The IXIM model, similar to the CERES (Fig. 3), calculates the thermal time with a capped linear function of the daily mean temperature. However, this approach fails to recognize that supraoptimal temperatures may reduce the maize development rate as other models do (Kumudini et al., 2014). We implemented the simplified beta function (Yan and Hunt, 1999) to estimate the effective daily thermal time (*TTd*):

$$TTd = TTx\left(\frac{Tx - T}{Tx - To}\right)\left(\frac{T}{To}\right)^{\frac{To}{Tx-To}} \quad (1)$$

where *TTx* is the maximum thermal time at the optimum temperature *To*, *T* is the daily mean temperature, and *Tx* is the maximum temperature at which the daily thermal time becomes zero. The function assumes a gradual curvilinear increase in thermal time between mean temperatures of zero and *To* and a corresponding drop between *To* and *Tx* (Fig. 3). In our implementation, the daily mean temperature is calculated by averaging the extrapolated hourly temperatures (Parton and Logan, 1981), forcing them within the limits of zero and *Tx*.

Many processes within IXIM, such as leaf expansion and senescence, are calculated over a thermal time basis. Changing the current range of thermal time values (by modifying the *TTx* value) would require recalibration of all the maize parameters within DSSAT. Previous studies discussing parameters such as the phyllochron (*e.g.*, Vinocur and Ritchie, 2001) would be meaningless. Our first concern when implementing Eq. (1) was to maintain a similar range of thermal time values while responding to the above optimal temperatures. For that reason, we first optimized the parameter *TTx* while maintaining constant *To* (32.1 °C) and *Tx* (43.7 °C) as determined by Kim et al. (2012) for the leaf tip appearance. We used the Simulated Annealing (SA) optimizer algorithm, as implemented by Goffe et al. (1994), which previously gave us good results (Lizaso et al., 2001; Soldevilla-Martinez et al., 2014). The optimizer minimizes an objective function, such as the sum of squares for the difference between simulated and observed values (phenology data of three sites, two sowing dates of 2015, see section "*Model calibration*"). Two optimization cycles were run to allow for different *TTx* values in the vegetative (sowing to anthesis) and reproductive (anthesis to maturity) periods. In the second step, parameters *To* and *Tx* were optimized while keeping *TTx* unchanged using the same field data and keeping the vegetative and reproductive stages separate. The result was two separate sets of optimized parameters for the vegetative phase and a corresponding set for the reproductive phase.

2.3.2. Calculating a heat stress index

We hypothesized that a certain interval within the daytime period is more directly related to the impact of heat on pistillate flowers, pollen viability, and pollination in maize. A time window between 3 h after dawn and 3 h before sunset was used to examine the hourly temperatures as follows:

$$HB = \left(14 - \frac{DayL}{2}\right) + 3 \quad (2)$$

$$HE = \left(14 + \frac{DayL}{2}\right) - 3 \quad (3)$$

where *HB* and *HE* are the hour to begin and to end checking the extrapolated hourly temperatures, respectively, and *DayL* is the model calculated daylength (hours). Eqs. (2) and (3) assume that the daytime hours are equally distributed around 2:00 p.m. (solar time). Therefore, every day, the model compares the hourly temperatures (*Th*) between *HB* and *HE*, against a critical temperature *Tc*, summarizing the information into a heat stress index (*HSI*; Challinor et al., 2005). When the temperature is greater than the *Tc*, the *HSI* value is calculated as follows:

$$HSI = 1 - \left(\frac{Th - Tc}{Tmx - Tc}\right) \quad (4)$$

where *Tmx* is the temperature at which kernel set is assumed to be zero. The *HSI* is bounded between zero and one, assigning a value of one to the hours with *Th* values under the *Tc*. When the average *HSI* for the hours between *HB* and *HE* is calculated, this value measures the heat stress intensity during the day, yielding lower values with higher temperatures.

In addition to the *HSI*, the model includes another provision to simulate the impact of heat stress, *i.e.,* the effect of extreme temperatures. When the model inspects hourly temperatures to identify temperatures above *Tc*, it also checks for temperatures reaching a maximum that can sterilize the pollen shed that day. That sterilizing temperature, or *Ts*, was set tentatively at 41 °C.

2.3.3. Simulating pollen shed, silk extrusion, and kernel set under heat

Previously, we developed procedures to simulate the dynamics of pollen emission and silk appearance in maize crops under non-stress conditions (Lizaso et al., 2003a, 2007). We adapted and complemented these procedures to simulate the impact of heat on the reproductive systems of maize. The flowering event in the current IXIM, as in CERES, is silking. Anthesis is not simulated. Both models assume that silking occurs when the flag leaf completes expansion (*i.e.*, the plant leaf is fully grown). In this study, we modified the IXIM model to simulate daily cohorts of plants that reached anthesis successively (the beginning of pollen shed) until the whole population was complete. The crop anthesis date is when 50% of the population begins pollen shed, which coincides with the completion of the leaf expansion period. Each day, the total number of plants shedding pollen (*PopSh*) is calculated as:

$$PopSh = Pop\frac{1}{1 + exp(-Msl\ (TT - TTant))} \quad (5)$$

Parameters *TT* and *TTant* are cumulative thermal times of each day and of the day when 50% of the population starts pollen shed (*i.e.*, the anthesis date), respectively. The *Msl* controls the slope of the function, and with it, the duration of pollen production in the field. Eq. (5) presumes a sigmoidal distribution of the plant population (*Pop*, plants ha^{-1}) that reaches anthesis. A crop that is growing under stress conditions increases the inter-plant variability at anthesis, and thus extends the period of pollen production (*i.e.*, *Msl* smaller). Rossini et al. (2011) showed the positive correlation between the early (V7-V10) shoot growth rate and the shoot growth rate around flowering, suggesting an early determination of the population heterogeneity close to anthesis. Therefore, using the Rossini et al. (2011) relationship and previously collected field data (Westgate et al., 2003; Fonseca et al., 2004), we developed two generic functions to estimate parameter *Msl* from the early shoot growth rate (*SGRe*, g $plant^{-1}$) as follows:

$$MALdur = 22.5\ SGRe^{-0.65} \quad (6)$$

$$Msl = 0.21\ MALdur^{-0.80} \quad (7)$$

where *MALdur* is the duration (days) of field pollen production (5–95% of population shedding pollen). Next, from Eq. (5), each cohort (*i*) of pollen-shedding plants is calculated:

$$NPopSh_i = PopSh - YPopSh \quad (8)$$

where *YPopSh* is the value of *PopSh* from the previous day and *i* is the specific cohort. The model keeps track of the pollen produced by each cohort *i* (*PG*, pollen grains $ha^{-1}\ day^{-1}$) during the time duration of the pollen shed from individual tassels (*Pdur*, days):

$$PG = NPopSh_i \frac{0.8\ PT}{0.3\ Pdur\sqrt{\frac{\pi}{2}}} \exp\left(-2\left(\frac{t - 0.5\ Pdur}{0.3\ Pdur}\right)^2\right) \quad (9)$$

The *PT* (grains $tassel^{-1}$) is the total pollen produced per tassel, and *t* (days) is each day within the *Pdur* time period. Eq. (9) follows a Gauss distribution of field pollen production (Lizaso et al., 2007), considering that 80% of the pollen released from the tassel reaches the level of the silks (Sadras et al., 1985). The pollen produced per cohort is algebraically transformed, using the plant density and *Pdur*, into the pollen rate (*Prt*, grains $cm^{-2}\ day^{-1}$) and then potential kernel set (*KSp*, %), as calculated with the Bassetti and Westgate (1994) function, is obtained:

$$\begin{aligned} KSp &= 0.96\ \text{Prt}, \quad 0 < Prt \leq 100 \\ KSp &= 96, \qquad\quad Prt > 100 \end{aligned} \quad (10)$$

The *KSp* value is multiplied by the heat stress index (*HSI*, Eq. (4)), yielding the expected daily percentage of kernel set as affected by heat (*KSi*):

$$KSi = KSp \times HSI \quad (11)$$

However, the calculated *KSi* can be further reduced if extreme temperatures are reached during the day:

$$KSFi = KSi \times (1 - 0.5\ NTs) \quad (12)$$

where *KSFi* is the final *KSi* stored for future use, and *NTs* is the number of hours with a temperature at or above *Ts*, which is indicative of pollen-sterilizing heat. Eq. (12) assumes that one hour at *Ts* reduces the kernel set by 50% and 2 h or more completely prevent fertilization.

The model estimates the thermal time to anthesis (*TTant*, Eq. (5)) at the end of the photoperiod-sensitive flower induction phase, once the number of differentiated leaves is known. By contrast, the time to silking (days) is only computed at the end of the critical time for kernel set, during the post-anthesis lag phase, when the anthesis-silking interval (ASI, see below) is calculated. Therefore, IXIM continues calculating the field pollen production and storing the heat-reduced kernel set (*KSi*, Eq. (11)) until no new cohort of plants shedding pollen is available. At the beginning of the effective grain filling, when the silking date has already been calculated, the dynamics of the plant population with silks and the corresponding kernel set are simulated.

The sequence of plants with exposed silks is estimated with a function analogous to that of Eq. (5), but working with days instead of thermal time. The model assumes a similar time duration of the population to complete the silking process (*FEMdur*, days) compared to the pollen shed process (*i.e.*, *FEMdur* = *MALdur*). Thus, the slope of the population with visible silks (*Fsl*) is:

$$Fsl = 9.25\ FEMdur^{-1.145} \quad (13)$$

Ears will extrude silks (*Sn*, number of exposed silks ear^{-1}) following a monomolecular function (Lizaso et al., 2003a):

$$Sn = HSI \times ST\left(1 - \exp\left(-\frac{3}{Sdur}\ t\right)\right) \quad (14)$$

where *ST* is the total number of exposed silks per ear and *Sdur* is the duration (days) for individual ears to complete silk extrusion. The number of extruded silks is reduced under stresses such as heat (Rattalino-Edreira et al., 2011) and water (Turc et al., 2016). Silks were assumed to remain receptive during 6 days under non-stress conditions (Bassetti and Westgate, 1993). However, under heat conditions, we found evidence (Lizaso et al., 2017, this issue) in accordance with previous reports (Cicchino et al., 2010b; Rattalino-Edreira et al., 2011; Ordóñez et al., 2015) that the female flowering is also disrupted. This effect was incorporated by reducing the silk receptivity to a minimum of four days (the condition tested in our greenhouse experiments, Lizaso et al., 2017).

Every day, a percentage of the total number of receptive silks, both newly exposed and un-pollinated the previous day, is assumed to be fertilized (*KSi*, Eq. (11)) and eventually converted into kernels per plant.

In summary, IXIM has three procedures to estimate the kernel number with a focus on different mechanisms that affect the reproductive systems:

a Male-system approach: Describing the predominant negative impact of heat on male reproductive systems (Cicchino et al., 2010b; Rattalino-Edreira et al., 2011) and on the potential kernel set, as developed in this work.
b Female-system approach: The silking delay is described with respect to anthesis (extended ASI) resulting from stresses other than heat (drought, N deficit, and crowding), because heat is not expected to have a clear and marked effect on the ASI (Cicchino et al., 2010a; Rattalino-Edreira et al., 2011). This approach is developed in a study that we are currently completing.
c Balanced approach: This approach describes the kernel set resulting from growing conditions without a major limiting stress, as integrated into the shoot growth rate around anthesis and developed in Lizaso et al. (2011).

The IXIM version developed in this work selects the first approach to calculate the kernel number only when there are at least 1.75 heat hours (an hourly temperature above *Tc*, Eq. (4)) per day on average during the pollen shedding period. When this premise is not met, an average of the kernel numbers as calculated with the second and third approaches is used.

2.4. Additional components in IXIM

Similar to CERES, the IXIM model estimates the crop N demand using a phenology-driven function (Jones, 1983). Recently, we showed (Yakoub et al., 2017) that the IXIM performance improves when the crop N demand uses a growth-driven function, similar to that proposed by Plénet and Lemaire (2000), together with new N partitioning rules and target grain N concentrations. Hence, we incorporated these new

Table 2
New parameters used in IXIM to simulate the impact of heat stress on the maize crops, definitions, values used in this work and file sources from where the information originates.

Variable	Definition	Value	Read from
Tc (Eq. (4))	Critical temperature for heat stress index	35 °C	Species file
Tmx (Eq. (4))	Maximum temperature for heat stress index	45 °C	Species file
SilkR	Number of days silks remain receptive under adequate growing conditions	6 days	Species file
PollDur	Average duration of pollen shed in individual tassels	4 days	Ecotype file
SilkDur	Average duration of silk extrusion in individual ears	4 days	Ecotype file
PollN	Millions of pollen grains produced by tassel	3.6 mill	Ecotype file
SilkN	Number of silks that are potentially convertible to grain under optimum pollination conditions	G2	Cultivar file

developments into the present version.

Under stress conditions, such as drought and soil N deficit, the silking time is delayed with respect to the anthesis time, thus increasing the anthesis-silking interval (ASI). We are currently completing a study in which we will link the stress-induced growth reduction during the critical period for kernel set with the extended ASI in IXIM. These components were also incorporated into the IXIM version described here.

2.5. IXIM new inputs

The new model requires two new cultivar-specific parameters to simulate ASI. The first parameter *ASNS* (days) is the typical ASI for the cultivar under non-stress conditions. The parameter can be positive (anthesis before silking: protandry) or negative (silking before anthesis: protogyny). The second parameter *ASEN* (unit-less) accommodates the ASI-specific response of each cultivar to stresses. It is defined as the extension in ASI when the crop experiences a severe stress, resulting in an average shoot growth rate of 1 g plant^{-1} day^{-1} during the critical period for kernel set.

In addition, some new parameters (Table 2) are required to simulate the impact of heat on maize. Critical (*Tc*) and maximum (*Tmx*) temperatures as used in Eq. (4) and silk receptivity (*SilkR*) are read from the model Species file, since a large variation across cultivars is not expected in these variables. The amount of pollen produced per tassel (*PollN*) as estimated by tassel size (Fonseca, 2004) is read from the model Ecotype file, since some variation is expected across groups of cultivars (*e.g.*, old *vs.* new hybrids). A similar relative variation is expected over the duration of silk emission by pistillate flowers in individual ears (*SilkDur*) and the duration of pollen shed by staminate flowers in individual tassels (*PollDur*). These two parameters are also read from the Ecotype file. One special case is the number of silks (*SilkN*) that can develop into kernels upon successful pollination. We decided to use the current cultivar parameter *G2*, the potential number of kernels per ear, as an approximate substitute as read from the model Cultivar file.

2.6. Model calibration

A cross-validation approach (Efron and Gong, 1983) was applied to calibrate the model parameters. This approach has been used previously for model calibration (Gimplinger and Kaul, 2009; Thorp et al., 2007). The CERES model was calibrated by following the sequential approach described by Boote (1999), using the same data sets as in IXIM. As explained before, we changed the calculation of the daily thermal time in IXIM (Eq. (1)) to capture the impact of the above optimal temperatures on developmental processes more accurately. The phenology field data from 2015, our hottest year, with two sowing dates in each location, was used to optimize the parameters of Eq. (1) (as described in the section "*Improving phenology simulation for high temperatures*"). The field data from 2014 and 2016 were used to validate the phenology model. In a second phase of this study, we sequentially calibrated (Boote, 1999) the cultivar-specific parameters related to the growth and yield of the CERES and IXIM models with the field data from 2016, and we validated the model accuracy with the field data from 2014 and 2015.

2.7. Model evaluation

The ability of the CERES and new IXIM models to capture the variation in our data sets was assessed with several indices. The root mean-squared error (RMSE) evaluates the proximity between the observed and simulated values, indicating the fit of the model to the measurements:

$$RMSE = \sqrt{\frac{\sum_{i=1}^{n} (Si - Oi)^2}{n}} \quad (15)$$

where *Si* and *Oi* are a corresponding pair of simulated and observed values, respectively, and n is the number of observations.

The calculated RMSE was normalized on a percentage scale (%) using the observed mean ($\overline{O}$), and yielding the relative root mean-squared error, or RRMSE:

$$RRMSE = \frac{RMSE}{\overline{O}} \times 100 \quad (16)$$

The Willmott's index of agreement (Willmott, 1982) or parameter *d*, was calculated as:

$$d = 1 - \left[\frac{\sum_{i=1}^{n} (Si - Oi)^2}{\sum_{i=1}^{n} (|Si'| + |Oi'|)^2} \right] \quad (17)$$

where $Si' = Si - \overline{O}$ and $Oi' = Oi - \overline{O}$. The index is bounded between one and zero, with one representing perfect agreement.

The mean absolute error (MAE) provides a measure of error based on the absolute value of the deviations, rather than on the squared error:

$$MAE = \frac{\sum_{i=1}^{n} |Si - Oi|}{n} \quad (18)$$

Similar to the RMSE, the MAE values are in the same units as the variable that is being evaluated.

2.7.1. Sensitivity analysis

The overall stability of the new IXIM and the sensitivity of the outputs to the new parameters were examined using the first sowing from 2015 in Cordoba, the most southern location, and our hottest treatment. Two components of the new model were evaluated. In the first analysis, the three parameters of the optimized beta function, the *TTx*, *To*, and *Tx* (Eq. (1)) used to estimate the thermal time, were modified, one at a time, within a range of plus or minus 30%, and the corresponding phenological responses were registered. In the second analysis, we changed the default parameters that were linked to the calculation of the heat stress index (*Tc* and *Tmx*, Eq. (4)), pollen shed (*PT* and *Pdur*, Eq. (9)), and silk extrusion (*ST* and *Sdur*, Eq. (14)) in a similar way, recording the responses in terms of the yield, yield components, and biomass at harvest.

Table 3
Optimized parameters of the simplified beta function (Eq. (1)) used to calculate the daily thermal times, with definitions and units.

Phase	TTx	To	Tx
Sowing – Anthesis	16. 28	30.04	47.63
Anthesis – Maturity	15.20	24.95	46. 94

TTx	Effective thermal time at To	Growing degree-days
To	Optimum temperature for maximum development rate	°C
Tx	Maximum temperature at which the development rate becomes zero	°C

3. Results

3.1. Field experiments

3.1.1. Phenology

Two different developmental thermal responses for the vegetative and reproductive periods (Fig. 3, Table 3) emerged after the parameters of the simplified beta function were optimized (Eq. (1), Yan and Hunt, 1999). Our data set (Table 4) included six growing seasons at three sites with a clear temperature gradient and more than 5% of the supraoptimal daily mean temperatures. Interestingly, the maximum temperature (*Tx*) and the maximum thermal time at the optimum temperature (*TTx*) of both phases were very close (Table 3). The primary difference was the optimum temperature (*To*), which was approximately 30 °C for the sowing-anthesis period, compared to 25 °C for the anthesis-maturity period.

After the calibration of cultivar coefficients (Table 5), both models adequately simulated (Fig. 4) the crop phenology for the years 2014 and 2016, with CERES and IXIM exhibiting RMSEs of 7.9 and 2.8 days (12.3 and 4.4% as RRMSE) for silking and 13.7 and 7.3 days (11.8 and 6.3% as RRMSE) for maturity, respectively (Table 6). All the statistical indices indicated that the IXIM model, which was equipped with the beta function, simulated the phenological events more accurately than the CERES model.

3.1.2. Grain yield and biomass accumulation

The new IXIM model, which was furnished with procedures to simulate the field dynamics of the pollen and silks as well as the impact of heat disrupting the pollination process, provided a small but consistent improvement in the grain yield simulations. The relative errors as indicated by the RRMSE were 15.9 and 14.1% for the CERES and IXIM models, respectively (Table 6), while the *d* parameter (Willmott, 1982) showed values of 0.84 and 0.92 (Table 6). It should be noted that our validation data set included 12 seasons, combining three sites with a strong thermal gradient, with two years and two sowing dates. All of them provided an ample range of thermal environments. A better estimation of the kernel numbers (Fig. 5 and Table 6) explained most of the enhancements in the IXIM grain yield estimates. Our field measurements of the kernel weights moved within a very narrow range, which was overestimated by both CERES and IXIM with very small *d* values of 0.12 and 0.16, respectively.

CERES underestimated the biomass accumulated over the growing season in most cases (Fig. 5). The biomass estimates from IXIM were substantially improved. Indices based on squared differences (RMSE) or on absolute differences (MAE) indicated errors of 6444 and 5877 kg ha^{-1} for CERES compared to 2645 and 2297 kg ha^{-1} for IXIM, respectively (Table 6).

Table 4
Frequency distribution of daily mean temperatures during the 2015 growing season used for the parameter optimization of the simplified beta function (Yan and Hunt, 1999). Data were collected from three sites with definite temperature gradients, and there were two sowing dates for each location.

Range of mean temperature (°C)	Frequency (%)
< 10	0.0
10–20	31.7
20–30	63.2
30–40	5.2
> 40	0.0
Minimum mean temperature:	12.5 °C
Maximum mean temperature:	32.4 °C

3.2. Greenhouse experiments

3.2.1. Phenology

The same cultivar coefficients that were calibrated with the field experiments (Table 5) were used to simulate the greenhouse experiments. CERES simulated the silking date with a mean error of 7 days, while IXIM had a mean error of 2 days according to the RMSE and MAE indices (Table 7). The flowering dates simulated by CERES were spread over a much larger range (47–68 DAS) than they were during the observed dates (51–60). By contrast, IXIM captured the range of silking dates (52–58) that were closer to the measured values (Fig. 6). Since the determination of the maturity date requires the destructive sampling of ears, we did not evaluate this variable in our greenhouse experiments.

3.2.2. Grain yield and yield components

In the greenhouse, the plants were subjected to extreme heat conditions, and CERES over represented the negative impact of these extreme conditions on the grain number and grain yield of the apical ears (Fig. 7). For the grain yield, the relative error (RRMSE) was on the order of 50% with mean errors of approximately 2.5 Mg ha^{-1} as shown by the RMSE and the MAE. However, IXIM mostly captured the general trend of the treatment effects on the grain yields with a relative error of 21% and mean errors of approximately 1.0 Mg ha^{-1} (Table 7).

The relative errors simulating the kernel number were 45% for CERES and 32% for IXIM (Table 7). The errors were traced back mostly to the failure to make a perfect estimation of the flowering time (Fig. 6). By contrast, the calculated kernel weights were closer to the measurements (Table 7) with relative errors between 25 (CERES) and 30% (IXIM).

3.3. Sensitivity analysis

Our first analysis examined the new calculation of thermal times (Fig. 8). We used two sets of parameters to calculate the thermal time with Eq. (1), with one for the sowing-anthesis phase and the other for the anthesis-maturity phase. Therefore, the relative responses in terms of anthesis and silking dates reported in Fig. 8 correspond to changes in the first set of parameters, while the maturity date results arose from variations in the second set of parameters. The model exhibited greater sensitivity to parameter changes during the vegetative phase (Anthesis, Silking) compared to the reproductive phase (Maturity). This response may be associated with the impact of the thermal time on the leaf appearance rate (Lizaso et al., 2003b) and the thermal time required for leaf expansion before anthesis. An interesting case was observed for the optimum temperature (*To*). As discussed earlier, *To* was the major difference in the beta function parameters between the vegetative and reproductive phases (Table 3), and it determines the temperature at which the maximum development rate occurs. Reducing the *To* from 30 to 21 °C (−30%) caused the anthesis to be simulated 5 days earlier (−8%). However, increasing the *To* from 30 to 39 °C (+30%) caused a delay of 53 days (+87%) in the anthesis date. The optimization procedure seems to have found the limit at which the changes started to have a relevant effect on the anthesis date.

Changes in the parameters of the beta function that affect the post-anthesis phase had minor effects on the simulated maturity date. The only exception was the maximum thermal time (*TTx*) at the optimum

Table 5
Calibrated cultivar parameters for the maize hybrid PR37N01 used in this study, with definitions and units.

Model	P1	P2	P5	G2	G3	PHINT	AX	LX	ASNS	ASEN
CERES	245.0	0.0	705.0	625.0	10.00	45.00	–	–	–	–
IXIM	225.0	0.0	830.0	615.0	9.25	38.00	850.0	980.0	−1.0	3.0

P1	Thermal time from emergence to the end of the juvenile phase	degree-days
P2	Photoperiod sensitivity, expressed as the additional duration of flower induction for each hour of increase above the critical photoperiod (12.5 h)	days
P5	Thermal time from silking to physiological maturity	degree-days
G2[a]	Maximum number of kernels per plant	kernels plant^{-1}
G3	Potential kernel filling rate during the linear grain filling stage	mg day^{-1}
PHINT	Thermal time interval between successive leaf tip appearances	degree-days
AX	One-sided surface area of the largest leaf	cm^2 leaf^{-1}
LX	Longevity of the most long-lived leaf in thermal time	degree-days
ASNS	Days between 50% anthesis (anthers visible) and 50% silking (stigmas visible) under non-stress conditions. The value could be positive (anthesis first: protandry) or negative (silking first: protogyny)	days
ASEN	ASI sensitivity to stresses. The number of days ASI is increased under a strong stress during the critical period for kernel set, producing an average shoot growth rate of 1 g plant^{-1}. Must be > =1	days

[a] G2 in IXIM is defined as the maximum number of kernels in the apical ear.

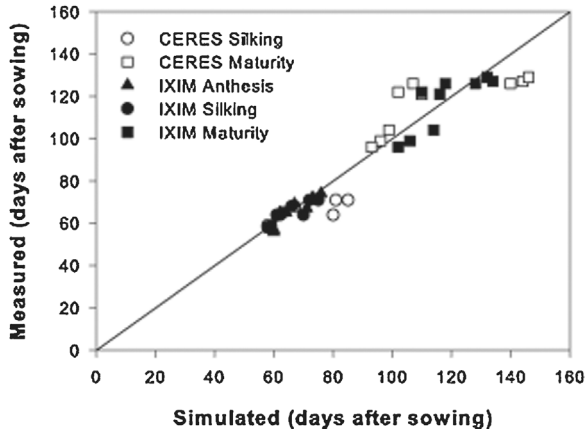

Fig. 4. Observed and simulated dates of anthesis, silking, and maturity by two maize models, CERES and IXIM. The field observations included two years (2014 and 2016; a total of three sowing dates) and three locations in northern, central, and southern Spain with a thermal gradient.

Table 6
Statistical indices to assess the accuracy of the simulations with the maize models CERES and IXIM. The indices were calculated by including only the validation data from the field experiments.

Variable	Model	RMSE	RRMSE	d	MAE
Anthesis	CERES	–	–	–	–
	IXIM	2.7	4.1	0.95	2.4
Silking	CERES	7.9	12.3	0.73	5.1
	IXIM	2.8	4.4	0.93	2.1
Maturity	CERES	13.7	11.8	0.82	12.1
	IXIM	7.3	6.3	0.89	6.7
Yield	CERES	1218.9	15.9	0.84	999.9
	IXIM	1082.1	14.1	0.92	895.2
Kernel Number	CERES	110.4	23.3	0.47	86.9
	IXIM	58.6	12.4	0.80	51.7
Kernel Weight	CERES	120.8	35.8	0.12	103.5
	IXIM	84.7	25.1	0.16	76.6
Biomass	CERES	6444.3	29.3	0.37	5877.2
	IXIM	2645.1	12.0	0.69	2297.5

temperature. Reducing the parameter by 30% from 16.3 to 11.4 GDD delayed the maturity by 29 days (27%), since each day accumulated less thermal time. However, increasing the *TTx* by 30%, from 16.3 to 21.2 GDD accelerated the reproductive phase reducing the maturity date by 12 days (−11%).

In the second analysis, we explored the simulation of the yield, yield components, and growth. Changes in the parameters used to calculate the heat stress index (HSI, Eq. (4)) and the pollen (Eq. (9)) and silks (Eq. (14)) dynamics had a significant effect on the grain yield and kernel numbers (Fig. 9). Our results documented the importance of the critical temperature (*Tc*) selection for calculating the heat stress index. A 30% decrease in the *Tc* (from 35 to 24.5 °C) resulted in a 53% reduction in the kernel numbers and grain yield. On the other extreme, sliding the *Tc* up by 30% (from 35 to 45.5 °C) enhanced kernel set and grain yield by 44% due to the absence of the above optimal temperatures.

Another interesting finding of our analysis is the negligible effect of the ± 30% variations in the number of pollen grains per tassel (*PT*, Eq. (9)), while the number of silks per ear (*ST*, Eq. (14)) exhibited a linear response in the kernel number and grain yield (Fig. 9). This finding suggests that just an approximate appraisal of the pollen amount based on the tassel size (Fonseca, 2004) combined with a more accurate estimate of the cultivar potential grain number under non-stress conditions (parameter *G2*, Table 5), as a surrogate for *ST* (Eq. (14)), might be sufficiently detailed for the input requirement in this new version of IXIM.

4. Discussion

The purpose of this work was to improve the predictive capacity of the IXIM model to simulate the impact of heat on the development, growth, and grain production of maize crops. The CERES model acted as a benchmark for comparison. Our first concern was the simulation of crop phenology. The former IXIM model (and also CERES) calculated the thermal time as a linear function of the daily mean temperature within the range of 8–34 °C (Fig. 3). At supraoptimal temperatures (> 34 °C), the thermal time remained constant as at 34 °C. However, a number of studies (*e.g.*, Parent and Tardieu, 2012; Yan and Hunt, 1999) show that the above optimal temperatures reduce the rate of development. Similarly, the need to use crop models for global change studies implies the simulation of temperature effects that are not often measured yet. To improve the calculated thermal time, we had to incorporate a function to reduce the development rate at supraoptimal temperatures.

Kumudini et al. (2014) compared a number of maize developmental functions in response to the temperature. In spite of the large data set used to test these functions, all the experiments came from the US Corn Belt and from Balcarce, Argentina, in the southern hemisphere, but with a similar latitude to the southern Corn Belt. As expected, and as the authors acknowledged, limited data involved above optimal temperatures (none mean daily temperature > 30 °C). Among the thermal

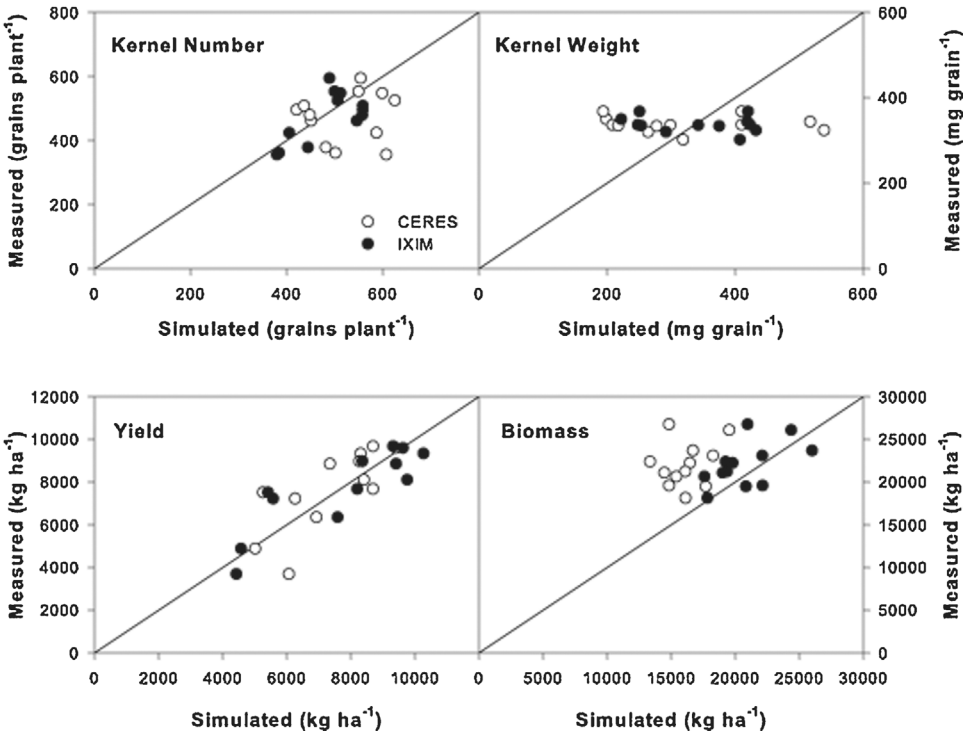

Fig. 5. Observed and simulated values of the kernel number, kernel weight, grain yield, and biomass at harvest. The field observations included two years (2014 and 2015; a total of four sowing dates) and three locations in northern, central, and southern Spain with a thermal gradient.

Table 7
Statistical indices to assess the accuracy of the simulations with the maize models CERES and IXIM. The indices were calculated using all the data (20 treatments over three years) from the greenhouse experiments.

Variable	Model	RMSE	RRMSE	d	MAE
Anthesis	CERES	–	–	–	–
	IXIM	2.6	4.7	0.64	1.8
Silking	CERES	7.4	13.3	0.46	7.0
	IXIM	2.6	4.6	0.61	1.9
Yield	CERES	2827.2	50.8	0.68	2478.8
	IXIM	1165.0	21.0	0.97	861.4
Kernel Number	CERES	152.5	45.5	0.63	132.3
	IXIM	106.8	31.8	0.92	89.4
Kernel Weight	CERES	80.6	24.8	0.79	63.6
	IXIM	96.4	29.7	0.77	77.1

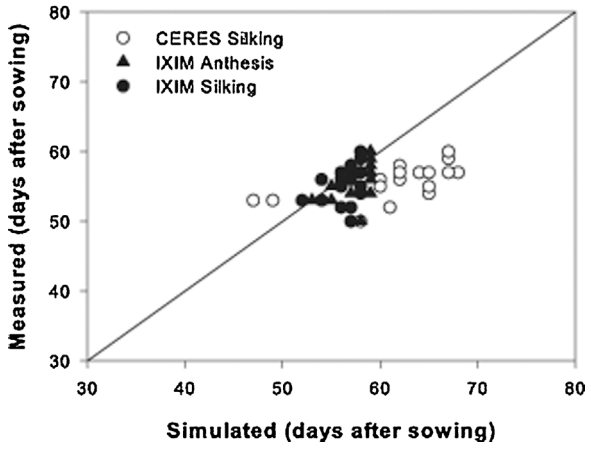

Fig. 6. Observed and simulated values of anthesis and silking by two maize models, CERES and IXIM. The greenhouse observations included a total of 20 treatments over three years growing in two chambers with daytime target temperatures of approximately 25 and above 35 °C.

functions compared here, they also tested the simplified beta function (Yan and Hunt, 1999). Interestingly, when the parameters of the beta function were optimized, the accuracy of the function improved.

In this study, we incorporated the simplified beta function into the IXIM model (Yan and Hunt, 1999) and optimized the function parameters. The hottest year of our available data (Table 4) was used for optimization, including 36 days (5.2%) with mean temperatures above 30 °C. Greenhouse data are frequently used to build new algorithms and find new model parameters. In this study, we succeeded in adjusting the parameters using field data, and this adjustment was shown to be precise enough to improve our capacity to simulate plants under fully different environments considerably, including our greenhouse experiments. With the optimized parameters, the function accumulated thermal time during the vegetative phase (data not shown), similarly to the MAIZESIM model (Kim et al., 2012) and to the GTI (Stewart et al., 1998) procedure. MAIZESIM had an optimum temperature of 31.2 and the polynomial GTI of 32.2 °C compared to our 30.04 °C. These optimum temperatures are in close agreement with the optimum temperature for leaf initiation and shoot growth (31.1 °C), as reported in the review by Sánchez et al. (2014). The optimum temperature as optimized for the reproductive phase decreased to 25 °C (Table 3), similar to the optimum for the grain-filling phase (26.4 °C) reported by Sánchez et al. (2014). Calculating the thermal time for the reproductive phase has to address the uncertainty associated with the assessment of physiological maturity. In a maize ear, there is a kernel maturity gradient from the base to the apex. In addition, the black layer formed at the base of the kernel, which is recognized as an indicator of crop maturity, actually shows that the kernel has already reached maturity, but it remains unclear when maturity was reached. We reduced this uncertainty by frequent ear sampling and by monitoring the grain growth of the mid-section of the ear until the final kernel size was reached. Our results (Fig. 4, Table 6) document the improved ability of IXIM to simulate crop maturity.

A second issue was the impact of heat on pollen viability, kernel set, and grain yield. Our approach was to introduce the simulation of plant cohorts that were shedding pollen and the corresponding cohorts of silk-extruding plants. The basic procedures were developed and tested previously (Lizaso et al., 2003a; Lizaso et al., 2007). The algorithms,

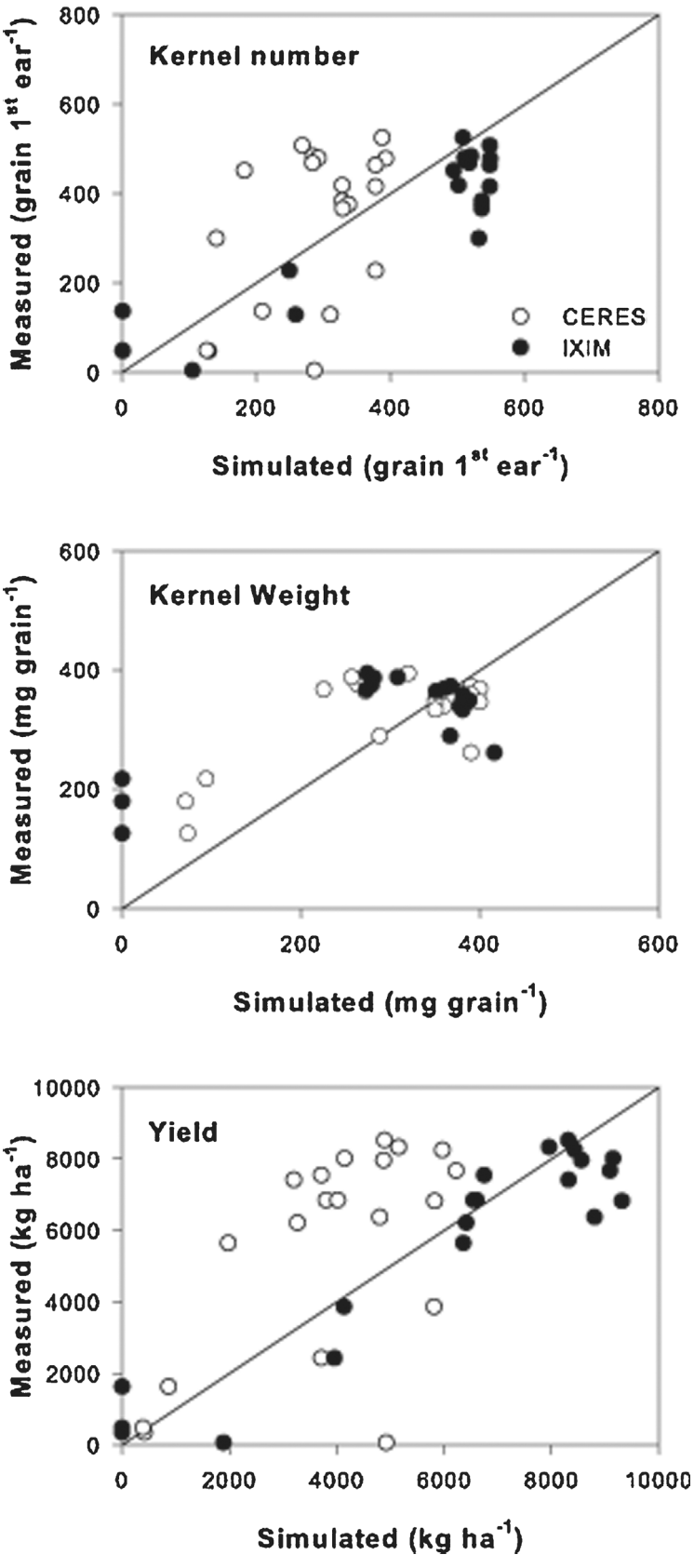

Fig. 7. Observed and simulated values for the kernel number, kernel weight, and grain yield of hand-pollinated apical ears. The greenhouse observations included a total of 20 treatments over three years growing in two chambers with daytime target temperatures of approximately 25 and above 35 °C. Circles indicate the 2014 and 2016 heat treatment at anthesis (see text).

which were developed for male and female inbreds in seed production fields, were adapted to simulate male and female flowering in grain maize fields. A heat stress index that incorporated the heat intensity above a threshold temperature (*Tc*, Eq. (4)) embodied the effect on the pollination and kernel set. This index was modified from Challinor et al. (2005) to include the period of the day that was more closely related to the pollen release. The effect of extreme temperatures was also included, assuming that pollen viability may be lost rapidly when

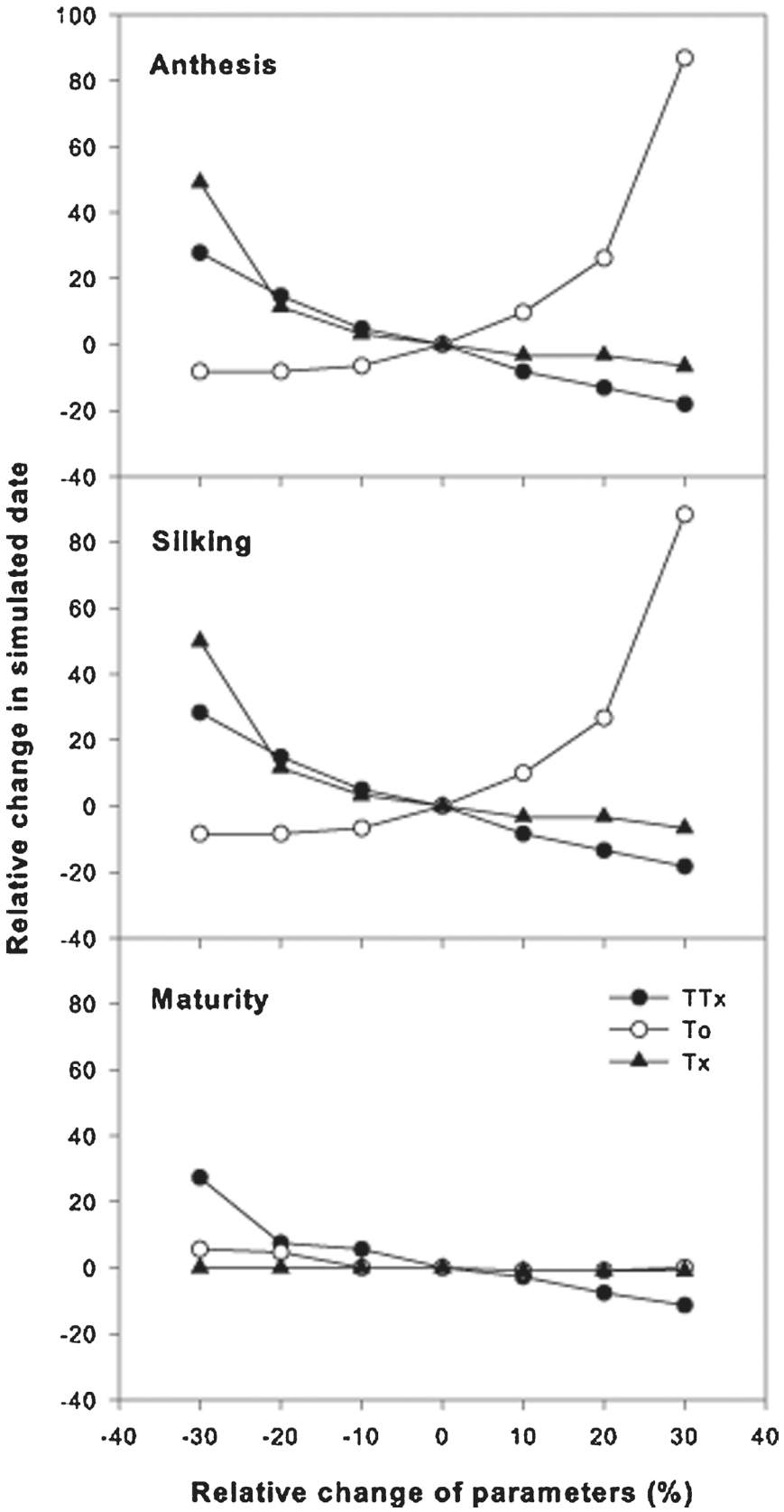

Fig. 8. Sensitivity analysis of the phenology components from the IXIM model developed in this study. The relative changes of the simplified beta function (Yan and Hunt, 1999, Eq. (1)) parameters were as follows: *To* (optimum temperature); *Tx* (maximum temperature); and *TTx* (thermal time at the optimum temperature).

exposed to extreme heat (Cicchino et al., 2010b; Rattalino-Edreira et al., 2011).

The threshold temperature for heat stress in maize is still an unresolved issue. Early work by Herrero and Johnson (1980) with excised tassels suggested that the *Tc* might be somewhere between 32 and 38 °C for various genotypes. More recently, Cicchino et al. (2010a) estimated the *Tc* to be 33.9 °C, which was the average from two field experiments on plants that were sheltered under polyethylene film to develop heat.

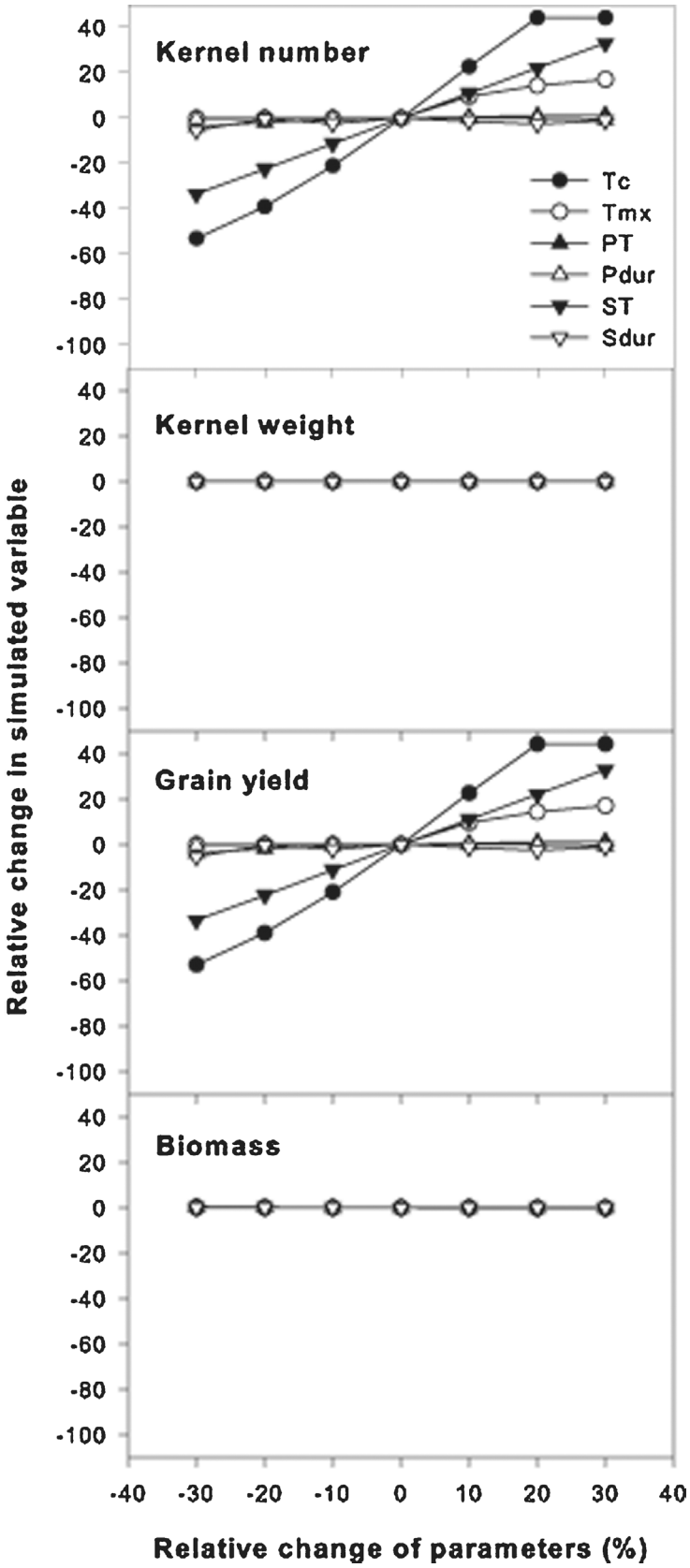

Fig. 9. Sensitivity analysis of the grain yield and growth components of the IXIM model developed in this study. The relative changes in the following parameters are included: *Tc* and *Tmx* (Eq. (4) calculating heat stress index); *PT* and *Pdur* (Eq. (9) calculating pollen shed); *ST* and *Sdur*, (Eq. (14) calculating silk extrusion).

Using a similar heating system, but with enhanced temperature control, Rattalino-Edreira et al. (2011) showed that a tropical genotype exhibited greater comparative advantages to endure heat than a temperate genotype. Sánchez et al. (2014) reviewed this issue and proposed 37.3 °C as the maximum temperature for pollination. We decided to use a more conservative *Tc* value of 35 °C to determine the threshold for heat damage to pollen and fertilization. The new procedures in IXIM substantially improved the simulation of kernel numbers in the field

experiments (Fig. 4, Table 6) compared to the CERES simulations. In the case of the controlled environment, the results were not consistent, since the short time window during which experimental heat was applied required extreme accuracy in the phenology estimates, which, in spite of improvements, were not always attained. This high accuracy will be critical in future model developments, because brief episodes of heat shock temperatures are expected to increase (IPCC, 2014) and have devastating consequences on male maize reproductive systems and the final kernel set (Herrero and Johnson, 1980; Cicchino et al., 2010b; Rattalino-Edreira et al., 2011). The enhanced kernel number simulation was reflected partially in the grain yield estimates, in part because of the biased calculation of the kernel weight (Fig. 5, Table 6). The difference in the yield simulation between both models was stronger when only the hottest environments in the validation data set were included in the analysis (*i.e.*, the southern location in 2014–15). In this case, the RMSE of CERES increased to 1403.9 kg ha^{-1}, while for IXIM, it remained at 1125.3 kg ha^{-1} (not shown).

The IXIM model estimates separated the impact of the temperature on the rates of instantaneous leaf photosynthesis and canopy respiration (Lizaso et al., 2011). These temperature functions seemed adequate under the conditions of our data sets. Recently, we incorporated new procedures to estimate the crop N demand and N partitioning, linking the crop C and N cycles closely (Yakoub et al., 2017). The biomass results (Table 6 and Fig. 5) add evidence supporting the better performance of IXIM growth simulations obtained after introducing these developments compared to the CERES simulations.

5. Conclusions

The available evidence indicates that surface temperatures will continue to increase and so will the frequency of extreme events such as heat waves. However, many of our crop simulation models do not correctly simulate the impact of these extreme events on crop development, growth, and production. In this study, we addressed this issue by improving the CSM-IXIM maize model to describe the effects of the above optimal temperatures on the phenology and male and female reproductive systems. We also incorporated the effects of extreme temperatures on the annihilation of the kernel set.

The simplified beta function, with parameters being optimized separately for the pre-anthesis and post-anthesis phases, improved the accuracy of the predicted phenological events when compared to CERES. The simulation of plant cohorts that reached anthesis and silking provided a platform to estimate the effects of timing and intensity of heat precisely. Two types of effects were accounted for as follows: i) the cumulative effect due to heat exposure above a critical temperature (*i.e.*, 35 °C), and ii) the shock effect due to exposure to extreme temperatures (*i.e.*, 41 °C). As a result of these new developments, the IXIM-simulated grain yield, yield components, and final biomass were closer to the measured values than the CERES-simulated variables, except for the kernel weight of the greenhouse experiments. In fact, the average kernel weight was always poorly estimated by both models.

This study extended the climatic range of previous field works. Many of the current uncertainties in our understanding of maize responses to heat stress, such as the determination of critical and extreme temperatures, should be addressed by collecting additional field data sets under a wider range of latitudes and thermal environments, including locations with the frequent occurrence of supraoptimal temperatures.

Acknowledgements

The authors are grateful for the financial support for this study from the MULCLIVAR project from the Spanish *Ministerio de Economía y Competitividad* (MINECO)CGL2012-38923-C02-02.; from the Spanish National Institute for Agricultural and Food Research and Technology (INIA, MACSUR01-UPM) through FACCE MACSUR - Modelling European Agriculture with Climate Change for Food Security, a FACCE JPI knowledge hub; and from the SUSTAg project (INIA, 652915 ERA-NET co-funded by FACCE-SURPLUS).

References

Bassetti, P., Westgate, M.E., 1993. Senescence and receptivity of maize silks. Crop Sci. 33, 275–278.
Bassetti, P., Westgate, M.E., 1994. Floral asynchrony and kernel set in maize quantified by image analysis. Agron. J. 86, 699–703.
Boote, K.J., 1999. Concepts for calibrating crop growth models. In: In: Hoogenboom, G., Wilkens, P.W., Tsuji, G.Y. (Eds.), DSSAT Version 3. A Decision Support System for Agrotechnology Transfer, vol. 4–6. University of Hawaii, Honolulu, HI, pp. 179–200.
Brown, D.M., Bootsma, A., 1993. Crop Heat Units for Corn and Other Warm Season Crops in Ontario. Ministry of Agriculture and Food, Guelph, ON, Canada.
Brown, D.M., 1969. Heat Units for Corn in Southern Ontario. Ministry of Agric. and Food, Guelph, ON, Canada.
Challinor, A.J., Wheeler, T.R., Craufurd, P.Q., Slingo, J.M., 2005. Simulation of the impact of high temperature stress on annual crops yields. Agr. For. Meteorol. 135, 180–189.
Cicchino, M., Rattalino Edreira, J.I., Otegui, M.E., 2010a. Heat stress during late vegetative growth of maize: effects on phenology and assessment of optimum temperature. Crop Sci. 50, 1431–1437.
Cicchino, M., Rattalino-Edreira, J.I., Uribelarrea, M., Otegui, M.E., 2010b. Heat stress in field-grown maize: response of physiological determinants of grain yield. Crop Sci. 50, 1438–1448.
Edmeades, G.O., Daynard, T.B., 1979. The relationship between final yield and photosynthesis at flowering in individual maize plants. Can. J. Plant Sci. 59 (3), 585–601.
Efron, B., Gong, G., 1983. A leisurely look at the bootstrap, the jackknife, and cross-validation. Am. Statistician 37 (1), 36–48.
FAO, 2014. FAO Statistical Databases. [Online]. Available at: http://www.fao.org/faostat/en/#data/QC.
Fonseca, A.E., Lizaso, J.I., Westgate, M.E., Grass, L., Dornbos Jr., D.L., 2004. Simulating potential kernel production in maize hybrid seed fields. Crop Sci . 44, 1696–1709.
Fonseca, A.E., 2004. Quantitative Assessment of Kernel Set and Risk of Out-Crossing in Maize Based on Flowering Dynamics. Iowa State University, Ames, Iowa PhD Dissertation.
Gimplinger, D.M., Kaul, H.-P., 2009. Calibration and validation of the crop growth model LINTUL for grain amaranth (*Amaranthus* sp.). J. Appl. Bot. Food Qual. 82, 183–192.
Goffe, W.L., Ferrier, G.D., Rogers, J., 1994. Global optimization of statistical functions with simulated annealing. J. Econometrics 60 (1), 65–99.
Herrero, M.P., Johnson, R.R., 1980. Drought stress and its effect on maize reproductive systems. Crop Sci. 21, 105–110.
Hoogenboom, G., Jones, J.W., Wilkens, P.W., Porter, C.H., Boote, K.J., Hunt, L.A., Singh, U., Lizaso, J.I., White, J.W., Uryasev, O., Ogoshi, R., Koo, J., Shelia, V., Tsuji, G.Y., 2015. Decision Support System for Agrotechnology Transfer (DSSAT) Version 4.6. DSSAT Foundation, Prosser, Washington. www.DSSAT.net.
IPCC, 2014. Climate change 2014: synthesis report. In: Core Writing Team, Pachauri, R.K., Meyer, L.A. (Eds.), Contribution of Working Groups I, II and III to the Fifth Assessment Report of the Intergovernmental Panel on Climate Change. IPCC, Geneva Switzerland, pp. 151.
Jones, C.A., Kiniry, J.R., 1986. CERES-Maize: A Simulation Model of Maize Growth and Development. Texas A & M Univ. Press, College Station.
Jones, C.A., 1983. A survey of the variability in tissue nitrogen and phosphorus concentrations in maize and grain sorghum. Field Crops Res. 6, 133–147.
Kim, S.-H., Yang, Y., Timlin, D.J., Fleisher, D.H., Dathe, A., Reddy, V.R., Staver, K., 2012. Modeling temperature responses of leaf growth, development, and biomass in maize with MAIZSIM. Agron. J. 104, 1523–1537.
Kumudini, S., Andrade, F.H., Boote, K.J., Brown, G.A., Dzotsi, K.A., Edmeades, G.O., Gocken, T., Goodwin, M., Halter, A.L., Hammer, G.L., Hatfield, J.L., Jones, J.W., Kemanian, A.R., Kim, S.-H., Kiniry, J., Lizaso, J.I., Nendel, C., Nielsen, R.L., Parent, B., Stöckle, C.O., Tardieu, F., Thomison, P.R., Timlin, D.J., Vyn, T.J., Wallach, D., Yang, H.S., Tollenaar, M., 2014. Predicting maize phenology: intercomparison of functions for developmental response to temperature. Agron. J. 106 (6), 2087–2097.
Lizaso, J.I., Batchelor, W.D., Adams, S.S., 2001. Alternate approach to improve kernel number calculation in CERES-maize. Trans. ASAE 44 (4), 1011–1018.
Lizaso, J.I., Westgate, M.E., Batchelor, W.D., Fonseca, A., 2003a. Predicting potential kernel set in maize from simple flowering characteristics. Crop Sci. 43, 892–903.
Lizaso, J.I., Batchelor, W.D., Westgate, M.E., 2003b. A leaf area model to simulate cultivar-specific expansion and senescence of maize leaves. Field Crops Res. 80, 1–17.
Lizaso, J.I., Batchelor, W.D., Boote, K.J., Westgate, M.E., 2005. Development of a leaf-level canopy assimilation model for CERES-Maize. Agron. J. 97, 722–733.
Lizaso, J.I., Fonseca, A.E., Westgate, M.E., 2007. Simulating source-limited and sink-limited kernel set with CERES-Maize. Crop Sci. 47, 2078–2088.
Lizaso, J.I., Boote, K.J., Jones, J.W., Porter, C.H., Echarte, L., Westgate, M.E., Sonohat, G., 2011. CSM-IXIM: a new maize simulation model for DSSAT version 4.5. Agron. J. 103, 766–779.
Lizaso, J.I., Ruiz-Ramos, M., Rodriguez, L., Gabaldon-Leal, C., Oliveira, J.A., Lorite, I.J., Sánchez, D., Garcia, E., Rodriguez, A., 2017. Impact of elevated temperatures in maize: phenology and yield components. Field Crops Res in this issue.
McCree, K.J., 1974. Equations for the rate of dark respiration of white clover and grain sorghum as function of dry weight, photosynthetic rate, and temperature. Crop Sci. 14, 509–514.

Mitchell, J.C., Petolino, J.F., 1988. Heat stress effects on isolated reproductive organs of maize. Plant Physiol. 133, 625–628.
Oberhuber, W., Edwards, G.E., 1993. Temperature dependence of the linkage of quantum yield of photosystem II to CO2 fixation in C4 and C3 plants. Plant Physiol. 101, 507–512.
Ordóñez, R.A., Savin, R., Cossani, C.M., Slafer, G.A., 2015. Yield response to heat stress as affected by nitrogen availability in maize. Field Crops Res. 183, 184–203.
Parent, B., Tardieu, F., 2012. Temperature responses of developmental processes have not been affected by breeding in different ecological areas for 17 crop species. New Phytol. 194, 760–774.
Parent, B., Turc, O., Gibon, Y., Stitt, M., Tardieu, F., 2010. Modelling temperature-compensated physiological rates, based on the co-ordination of responses to temperature of developmental processes. J. Exp. Bot. 61, 2057–2069.
Parton, W.J., Logan, J.A., 1981. A model for diurnal variation in soil and air temperature. Agric. Meteorol. 23, 205–216.
Plénet, D., Lemaire, G., 2000. Relationships between dynamics of nitrogen uptake and dry matter accumulation in maize crops. Determination of critical N concentration. Plant Soil 216, 65–82.
Rattalino-Edreira, J.I., Otegui, M.E., 2012. Heat stress in temperate and tropical maize hybrids: differences in crop growth, biomass partitioning and reserves use. Field Crops Res. 130, 87–98.
Rattalino-Edreira, J.I., Otegui, M.E., 2013. Heat stress in temperate and tropical maize hybrids: a novel approach for assessing sources of kernel loss in field conditions. Field Crops Res. 142, 58–67.
Rattalino-Edreira, J.I., Budakli-Carpici, E., Sammarro, D., Otegui, M.E., 2011. Heat stress effects around flowering on kernel set of temperate and tropical maize hybrids. Field Crops Res. 123, 62–73.
Ritchie, J.T., Singh, U., Godwin, D.C., Bowen, W.T., 1998. Cereal growth and development. In: Tsuji, G.Y., Hoogenboom, G., Thornton, P.K. (Eds.), Understanding Options for Agricultural Production. Kluwer Academic Publishers, Dordrecht, Netherlands, pp. 79–98.
Rossini, M.A., Maddonni, G.A., Otegui, M.E., 2011. Inter-plant competition for resources in maize crops grown under contrasting nitrogen supply and density: variability in plant and ear growth. Field Crops Res. 121, 373–380.
Sánchez, B., Rasmussen, A., Porter, J.R., 2014. Temperature and the growth and development of maize and rice: a review. Glob. Change Biol. 20, 408–417.
Sadras, V.O., Hall, A.J., Schlichter, T.M., 1985. Kernel set of the uppermost ear in maize: I. Quantification of some aspects of floral biology. Maydica 30, 37–47.
Schoper, J.B., Lambert, R.J., Vasilas, B.L., 1987. Pollen viability, pollen shedding and combining ability for tassel heat tolerance in maize. Crop Sci. 27, 27–31.
Soldevilla-Martinez, M., Quemada, M., López-Urrea, R., Muñoz-Carpena, R., Lizaso, J.I., 2014. Soil water balance: comparing two simulation models of different levels of complexity with lysimeter observations. Agric. Water Manage. 139, 53–63.
Stewart, D.W., Dwyer, L.M., Carrigan, L.L., 1998. Phenological temperature response of maize. Agron. J. 90, 73–79.
Thorp, K.R., Batchelor, W.D., Paz, J.O., Kaleita, A.L., DeJonge, K.C., 2007. Using cross-validation to evaluate CERES-Maize yield simulations within a decision support system for precision agriculture. Trans. ASABE 50 (4), 1467–1479.
Turc, O., Bouteillé, M., Fuad-Hassan, A., Welcker, C., Tardieu, F., 2016. The growth of vegetative and reproductive structures (leaves and silks) respond similarly to hydraulic cues in maize. New Phytol. 212, 377–388.
Vinocur, M.G., Ritchie, J.T., 2001. Maize leaf development biases caused by air-apex temperature differences. Agron. J. 93, 767–772.
Westgate, M.E., Lizaso, J.I., Batchelor, W.D., 2003. Quantitative relationships between pollen shed density and grain yield in maize. Crop Sci. 43, 934–942.
Willmott, C.J., 1982. Some comments on the evaluation of model performance. Bull. Am. Meteorol. Soc. 63, 1309–1313.
Yakoub, A., Lloveras, J., Biau, A., Lindquist, J.L., Lizaso, J.I., 2017. Testing and improving the maize models in DSSAT: development, growth, yield, and N uptake. Field Crops Res. 212, 95–106.
Yan, W., Hunt, L.A., 1999. An equation for modelling the temperature response of plants using only the cardinal temperatures. Ann. Bot. 84, 607–614.